remote sensing

Communication

Energetic Electron Precipitation via Satellite and Balloon Observations: Their Role in Atmospheric Ionization

Irina Mironova [1,*], Galina Bazilevskaya [2,3], Vladimir Makhmutov [2,4], Andrey Mironov [1] and Nikita Bobrov [1]

1 Faculty of Physics, St. Petersburg State University, 199034 St. Petersburg, Russia
2 Lebedev Physical Institute, Russian Academy of Science, 119991 Moscow, Russia
3 Skobeltsyn Institute of Nuclear Physics, Moscow State University, 119991 Moscow, Russia
4 Moscow Institute of Physics and Technology, National Research University, 117303 Moscow, Russia
* Correspondence: i.a.mironova@spbu.ru

Abstract: Information about the energetic electron precipitation (EEP) from the radiation belt into the atmosphere is important for assessing the ozone variability and dynamics of the middle atmosphere during magnetospheric and geomagnetic disturbances. The accurate values of energetic electron fluxes depending on their energy range are one of the most important problems for calculating atmospheric ionization rates, which, in turn, are taken into account for estimating ozone depletion in chemistry–climate models. Despite the importance of these processes for the high latitudes of middle atmosphere, precipitation of energetic electrons is still insufficiently studied. In order to better understand EEP and related processes in the atmosphere, it is important to have many realistic observations of EEP in order to correctly characterize their spectra. Invading the atmosphere, precipitating energetic electrons, in the range from tens of keV to relativistic energies of more than 1 MeV, generate bremsstrahlung, which penetrates into the stratosphere and is recorded by detectors on balloons. However, these observations can be made only when the balloon is at stratospheric heights. Near-Earth satellites, such as the polar-orbiting operational environmental satellites (POES), are constantly registering precipitating electrons in the loss cone, but are moving too fast in space. Based on a comparison of the results of EEP measurements on balloons and onboard POES satellites in 2003, we propose a criterion that makes it possible to constantly monitor EEP ionization at stratospheric heights using observations on POES satellites.

Keywords: energetic electron precipitation (EEP); NOAA POES satellite and balloon observations; EEP spectra; atmospheric response; ionization rates

Citation: Mironova, I.; Bazilevskaya, G.; Makhmutov, V.; Mironov, A.; Bobrov, N. Energetic Electron Precipitation via Satellite and Balloon Observations: Their Role in Atmospheric Ionization. *Remote Sens.* **2023**, *15*, 3291. https://doi.org/10.3390/rs15133291

Academic Editors: Ke Du, Ravi Varma and Ying Zhang

Received: 7 May 2023
Revised: 18 June 2023
Accepted: 23 June 2023
Published: 27 June 2023

1. Introduction

The outer radiation belt of the Earth is located at a distance of 3–6 Re and contains mainly trapped electrons with energies from several keV to several MeV, the fluxes of which can vary significantly, sometimes for as fast as several hours [1]. One of the important channels for the loss of electrons from the belt is precipitation into the atmosphere, when the adiabatic motion is disturbed under the action of perturbations, and the electrons fall into the loss cone [2,3]. Another loss channel may be the escape of electrons into the interplanetary medium through magnetopause shadowing [4]. The relative role of these processes in the dynamics of the radiation belt has not yet been studied enough.

An altitude of about 100 km, the Karman line [5], is traditionally taken to be a boundary layer of energetic electron precipitation (EEP) losts into the atmosphere. Precipitated electrons collide with molecules of air and induce increasing atmospheric ionization rates (formation of ion pairs per second). Ionization rates play a key role in production of reactive odd nitrogen (NO_x) [6] and odd hydrogen (HO_x) [7] in the atmosphere. Finally, EEP via production of ion pairs impacts middle atmosphere chemistry and dynamics and leads to ozone depletion [8–13]. To better understand this relationship, it is important to have realistic observations to properly characterize energetic electron precipitation [14] and atmospheric ionization rates [15,16], which are incorporated into chemistry–climate models.

One of the EEP observation methods is the measurement on balloons of bremsstrahlung generated by precipitating electrons in the altitudes of stratosphere [17–19]. In our previous studies [15,20], we estimated the ion pair production into the atmosphere based on the results of selected EEP balloon observations in Apatity (N67.55, E33.33, the McIlwain parameter L = 5.3). The launches are performed three times a week and a balloon can register EEP only when it is at a height where bremsstrahlung penetrates. In reality, EEP occurs much more frequently, so many cases of EEP were missed. To assess the impact of EEP on weather and climate, we should know the additional ionization that is created by all precipitation events occurring in the polar regions. In this regard, here, we compare the results of observations on balloons and on satellites of the NOAA POES, for which the study of EEP is one of the main tasks of the mission. Then, we try to reconstruct more fully the picture of EEP occurrence in the auroral region for 2003. The task of this study is to estimate the occurrence of EEP in the northern polar latitudes throughout the day.

2. Balloon and Sattelite EEP Observations

Energetic particles from the radiation belts are lost to the atmosphere through precipitation and can be observed by balloons into the atmosphere and by low-Earth orbiting (LEO), such as NOAA polar orbiting environmental satellites (POES). The combination of balloon observations with satellite measurements of energetic electron precipitation (EEP) gives a more complete picture of the precipitation of electrons from the radiation belt into the atmosphere.

EEP in the energy range from tens of keV to more than 1 MeV, generate bremsstrahlung, which penetrates into the stratosphere and can be recorded by detectors on balloons. These electrons are absorbed at altitudes above than 50 km, but generated bremsstrahlung X-rays penetrate into the atmosphere down to altitudes of about 20 km and can be detected by a balloon Geiger counter. Balloon measurements of ionizing radiation in the atmosphere, which have been performed by the Lebedev Physical Institute (LPI) in the Murmansk region for more than 60 years [21], allow us to observe the energetic electron precipitation from the outer radiation belt of the Earth.

The equipment detects secondary cosmic rays, as well as solar energetic particles and bremsstrahlung from precipitating magnetospheric electrons in case they enter the atmosphere. The technique makes it possible to separate these three types of radiation [17]. In the case of electron precipitation, we subtract from the instrument readings the background caused by secondary cosmic rays and obtain bremsstrahlung fluxes at different altitudes in the atmosphere. In 99% of cases, precipitation is observed at an altitude above 20 km [22]. In the absence of strong fluctuations, the dependence of bremsstrahlung fluxes on the residual atmospheric pressure (the so-called absorption curve) can be approximated by an exponential law and allows one to pass to the energy spectrum of precipitating electrons at the atmospheric boundary (Karman line [5]).

Taking into account the accuracy of determining the height of the balloon and the statistical errors in measuring the counting rate of the device, we estimate the total reliability of the estimate of bremsstrahlung fluxes as 50%. As already mentioned, the balloon launches are performed three times a week and we can register EEP only when it is at a height where bremsstrahlung penetrates. We register EEP at a given location at a given moment and we do not know the time of the beginning and end of the event. We determine the energy spectrum of the precipitating electrons from the absorption of bremsstrahlung in air during the ascent of the balloon. A correct estimate of the spectrum can only be obtained under the condition that the flux of precipitating electrons remained constant during the measurement time, which corresponds to a smooth increase in the counting rate of the device with increasing altitude. This condition is met in ∼30–50% of reported EEP cases, since in reality, variability in the precipitating electron flux values on a time scale from seconds to several hours with a typical characteristic time being on the order of minutes is their intrinsic feature [19,20,23]. However, even in those cases when the spectrum according to balloon measurements is not determined correctly, we can confidently state that EEP has taken place. The LPI catalog of precipitating electrons (http://sites.lebedev.ru/en/DNS_FIAN/479.html (last accessed on 18 June 2023)) contains all recorded events.

The NOAA POES satellites have proven valuable in understanding EEP [24,25]. POES measures electrons in several energy channels at an altitude of about 820 km. The medium energy proton and electron detectors (MEPED) instrument on board the POES spacecraft has two identical electron telescopes with solid-state detectors. At high latitudes, the 0° telescope measures precipitating electrons, while the 90° telescopes track particles trapped in the Van Allan radiation belts [24]. Thus, data from the 0° electron telescope are used to estimate electron precipitation in high-latitude regions, where the fluxes increase significantly during the period of geomagnetic disturbances. The EEP data were taken from the MEPED vertical telescope, which detects precipitating electrons at polar latitudes [24] in three energy channels, i.e., E1, E2, and E3, with electron energies >30, >100, and >300 keV, respectively. In addition, we took advantage of the fact that the P6 proton channel (>6900 keV) is contaminated with electrons with energies above ∼800 keV, while the P5 proton channel (2500–6900 keV) is free of electrons. This means that in the absence of a signal in the P5 channel, the P6 channel registers pure electrons with energies above ∼800 keV [25].

3. Method of Energetic Electron Precipitation Selection Based on Satellite and Balloon Observations

The comparison of balloon observations with satellite measurements was made for 2003, when there were three satellites (NOAA POES 15, 16, and 17) in orbit in near-Earth space, separated by ∼100 degree in longitude. The sun-synchronous orbit inclination angle was 98.7, altitude 822 km, and orbital period 101.5 min (mean values).

The difficulty of comparing the results of EEP measurements on balloons and on satellites is due to the rapid movement of satellites in orbit. During the flight, a balloon may move away from the site of launching as far as 100 km by longitude but not by latitude because of the wind direction in this region. The balloons register EEP within ∼5–40 min. POES satellites in the Apatity region pass in 1 min more than 3° in latitude and longitude, i.e., ∼341 and ∼155 km, respectively. Keeping in mind the coordinates of Apatity (N67.55, E33.33, the McIlwain parameter L = 5.3), we chose for comparison the data of satellites, the measurement time of which intersected with the measurement time on the balloons, geographic latitude of foot-of-field-line 66°–69°, geographic longitude of foot-of-field-line 10°–50°, and McIlwain parameter L = 4–8. Thirteen EEP events out of 25 registered by balloons in 2003 met these requirements. It turned out that in the case of detection of precipitation in the stratosphere, the electron fluxes on POES satellites in the P6 channel always exceeded 100 pfu [26].

Therefore, taking into account only those precipitations where the flux in the P6 channel was above 100 pfu with zero readings in the P5 channel should be considered the lower threshold at which the precipitation of relativistic electrons would be observed in the Murmansk region, Apatity if the balloon was constantly at the required height.

For our study, we used 16-s MEPED measurement results that met the following conditions: measurement time, 24 h a day, geographic latitude of foot-of-field-line, 60°–70°, geographic longitude of foot-of-field-line, 0°–360°, McIlwain parameter, L = 4–8, and P6 channel reading more or equal 100 pfu with zero P5 reading. The results of all three POES satellites that met the specified conditions were averaged over a day.

In fact, such EEPs were observed by satellites every day, but sometimes for a very short time. Therefore, for further analysis, we took only those days when the precipitation was observed for at least 320 s. We summarized the time of observation by three satellites per day and consider it as daily EEP duration at the north polar region.

It should be noted that this method does not work during the invasion of solar energetic particles, because proton channel P5 registers protons at this time. Therefore, the following days of 2003 were excluded from consideration: 148, 151, 169, 299–302, 306, 308, 324, 325, and 336 (http://www.wdcb.ru/stp/data/SPE/Catalog_SPE_23_cycle_SA.pdf (last accessed on 18 June 2023)). However, the absence EEP elsewhere—beginning at the first part of the year or around 200 and 250 days of year—means that there were no EEP that met the accepted selection criteria. Figure 1 shows the duration of the selected events according to the POES and the balloon observation. It can be seen that in 2003, in the northern auroral zone, 10 times more EEP cases could occure than was observed on balloons. According to this figure, the duration of EEP on balloons is longer than on satellites, but this is due to the too-fast passage of the satellites through the auroral zone.

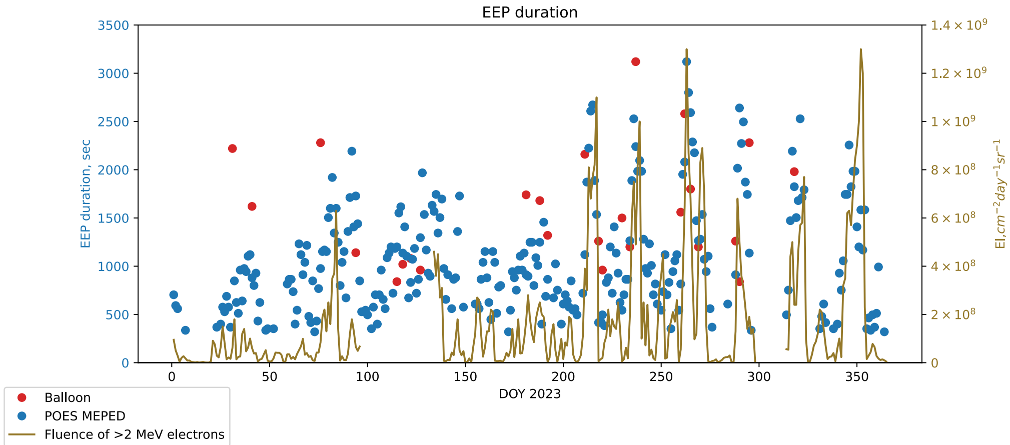

Figure 1. EEP duration observed by POES and balloon measurements. Red—balloon EEP duration; blue—MEPED POES spacecraft EEP duration. Line shows daily fluence of >2 MeV electrons in the outer radiation belt .

Figure 1 also demonstrates the dynamics of the fluence of relativistic electrons in the outer radiation belt of the Earth [27], (http://www.ngdc.noaa.gov/stp/solar/sateenvi.html (last accessed on 18 June 2023)). The reasonable consistency of EEP events distribution with variations in the electron fluence can be considered as an indication of the effectiveness of the proposed criterion for EEP selection.

4. Energy Spectra of Precipitating Electrons

To estimate ionization in the atmosphere, it is necessary to know the energy spectra of precipitating electrons. Various distributions use the fitting energy spectrum of energetic electron precipitation, such as the Maxwellian type of electron energy spectra distribution [28,29] or the exponential-law function of energy spectra distribution [3,29,30]. For describing EEP from outer radiation belt, the most common is the power-law distribution [29,31].

The Van Allan radiation belts [24]. transition from the bremsstrahlung fluxes recorded in the atmosphere to the fluxes of precipitating electrons on the Karman line was carried out on the basis of calculations by the Monte Carlo method [17]. Two forms of the spectrum of precipitating electrons were used in the calculations—exponential and power law. It turned out that the exponential spectrum in some cases leads to too-low bremsstrahlung fluxes in the atmosphere, which were inconsistent with observations. According to direct measurements of the high-energy electron precipitation [31], the power-law spectrum is observed most frequently. Therefore, we focused on the power spectrum. We fitted the data of the four POES channels to a power law. The reliability coefficient of this fitting for EEP events with P6 channel reading >100 pfu was $R^2 = 0.87$, $std = 0.16$. Then, we converted an integral spectrum into a differential one for comparison with the balloon data.

For this investigation, we use the power-law fitting of the energy spectra in the following form:

$$F(E) = A \cdot E^{-k}, \quad (1)$$

where $F(E)$ is the power-law energy spectrum, A is a parameter of the flux of incident electrons (cm^{-2} s^{-1} sr^{-1} keV^{-1}), and k is the spectral index.

In Figure 2, we give examples of spectra obtained on balloons and on satellites on the same day, at distances less than 1000 km between them. In the Van Allan radiation belts [24]. addition, the measurement data on the balloons satisfied the condition of the absence of significant temporal fluctuations. Note that Figure 2 shows the results of the calculated spectra in power-law form. Symbols set for the eye guide. Taking into account the strong variability of electron fluxes and the features of the observations described above, we can state a fairly good agreement between the fluxes and spectra of electrons shown in Figure 2. However, in other cases, quite significant discrepancies in the results are found, as evidenced by the scatter in the parameters of fitting the spectra obtained on the same day on balloons and satellites.

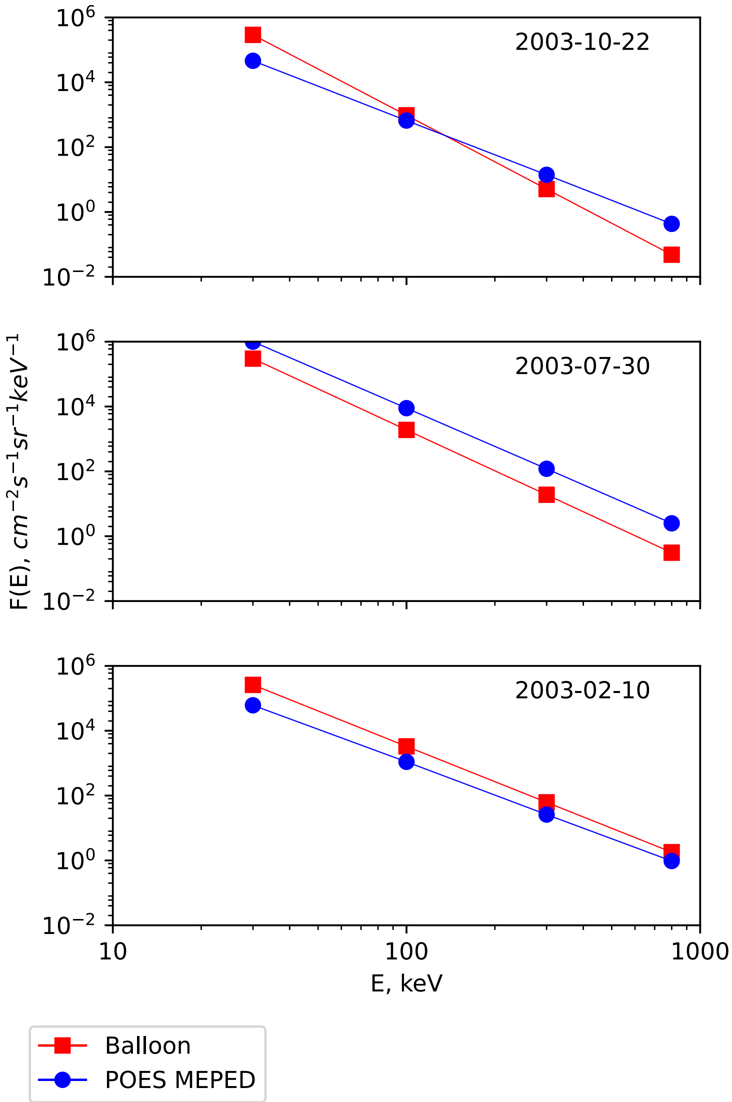

Figure 2. Examples of selected EEP energy spectra. Red—balloon EEP energy spectra; blue—MEPED POES spacecraft EEP energy spectra. Symbols set for the eye guide.

Figure 3 presents the data of all 25 cases of precipitation recorded by balloons in 2003. It can be seen that the scatter of the fitting parameters A and k from Equation (1) for balloon measurements is greater than for measurements on satellites. This means that in a number of cases, during measurements, strong temporal variations in electron fluxes existed. Nevertheless, we can state with certainty that an EEP events took place. The results of satellites are free from this shortcoming because the observation time is very short and they were used to estimate the ionization of the atmosphere at polar latitudes in 2003.

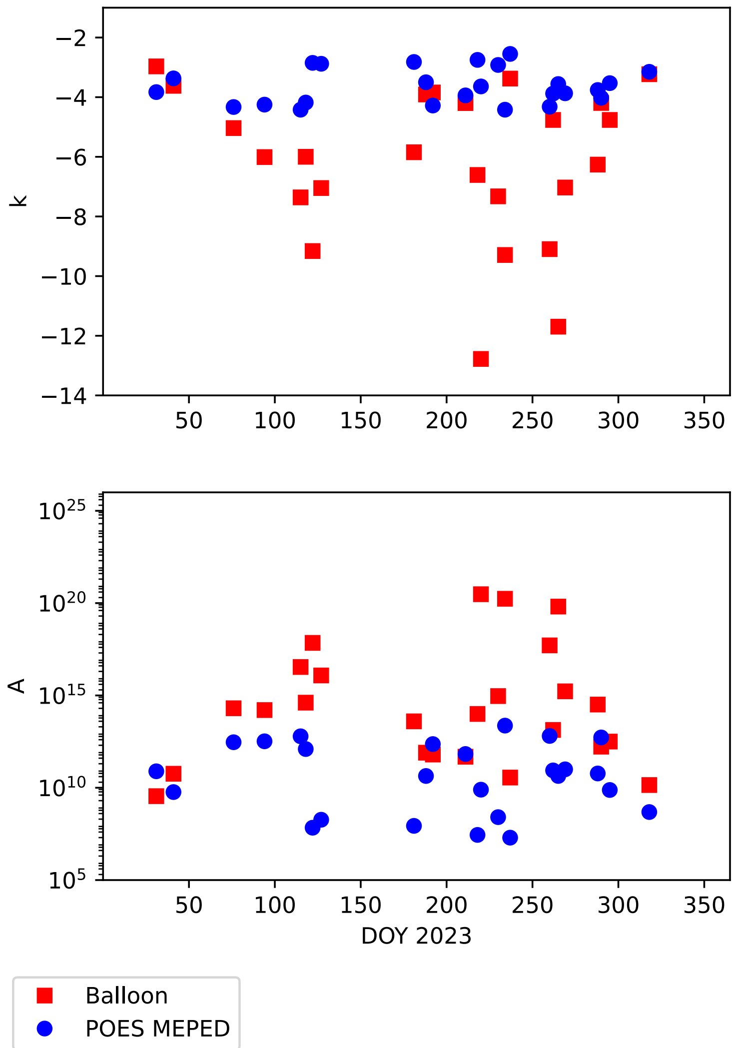

Figure 3. Satellite and balloon power law spectra parameters (described by Equation (1)) for all balloon observations in 2003. Red—balloon spectra parameters A and k; blue—MEPED POES spacecraft spectra parameters A and k.

5. Ionization Rates in the Atmosphere Based on EEP Observed by MEPED POES during 2003

In this study, we compute the ionization rates Q(h) (ion pairs g $^{-1}$ s $^{-1}$) as follows:

$$Q(h) = \int_{E_x}^{E_n} Y(h, E) \cdot F(E) dE, \tag{2}$$

where $F(E)$ is a spectral distribution (cm^{-2} s $^{-1}$ sr^{-1} keV^{-1}) of precipitating electrons at the top of atmosphere and E_x and E_n are the minimum and maximum energies of electrons in a flux. The calculation of the yield function $Y(h, E)$ is discussed in the recent paper [29].

The power-law integral energy spectra $F(E)$ are computed by Equation (1), fitting MEPED POES satellite EEP flux mesurements.

Figure 4 shows the distribution of ionization rates with height in the atmosphere for all cases of EEP in 2003 identified using the developed criterion according to the POES data. Figure 5 shows the distribution of ionization over time. During 2003, a strong variability of ionization rates by five orders of magnitude was observed in the upper atmosphere due to the strong variability of the EEP flux in the energy range below 100 keV. A lower variability (by three orders of magnitude) of the ionization rate is observed in the middle atmosphere of about 50 km, and the ionization rate changes by two orders of magnitude at a height of about 25 km. According to these results, EEP created a noticeable increase in atmospheric ionization at altitudes above 25 km for about 300 days in 2003. In fact, there were more of these days, since days of solar energetic particle intrusions are not taken into account here.

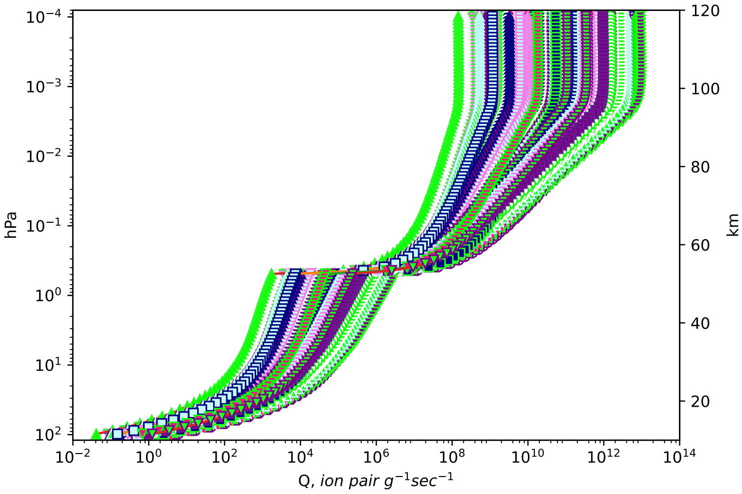

Figure 4. Vertical profile of ionization rates during selected EEP events observed by MEPED POES.

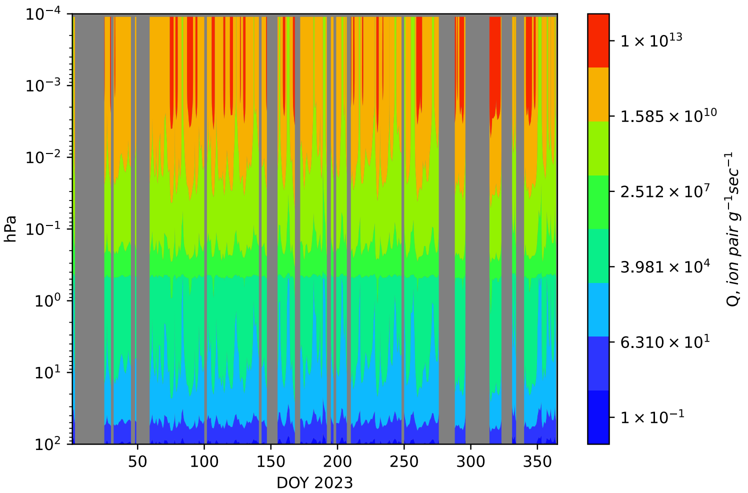

Figure 5. Vertical profile of ionization rates during selected EEP events observed by the MEPED POES satellite during 2003.

EEP is closely related to geomagnetic disturbances, although this relationship is complex, because it consists of many processes—energy supply and accumulation into the magnetosphere from the solar wind, development of various waves. and wave–particle interactions. As a result, both the acceleration of electrons and their entry into the loss cone occur. Ionization at the heights of the stratosphere is produced only by sufficiently strong

EEP. Therefore, it can be expected that there is a correlation of the obtained ionization rates from EEP on a planetary scale with some planetary geomagnetic indexes.

Figure 6 shows that EEP produces ion pairs depending on geomagnetic disturbances at the altitude of balloon observations about 25 km. The figure presents the scatter plot for the obtained ionization rates at a height of 25 km and Kp, Ap indices. The correlation coefficient is 0.70 ± 0.031 with the Kp index and 0.71 ± 0.030 with the Ap index. We conclude that on the days we selected according to the developed criterion, rather powerful EEP did occur. The correlation between geomagnetic disturbances and EEP arises because both phenomena are a consequence of the response of the magnetosphere to the effects of the dynamic solar wind. The conditions in the magnetosphere that contribute to the acceleration and loss of electrons are constantly changing, which leads to variability in the EEP fluxes for the same values of geomagnetic indices. Figure 6 shows a linear dependence on geomagnetic disturbances, the higher the level of disturbances, the greater the number of ion pairs in the atmosphere. The ionization rate of the stratosphere is very small, but still exists.

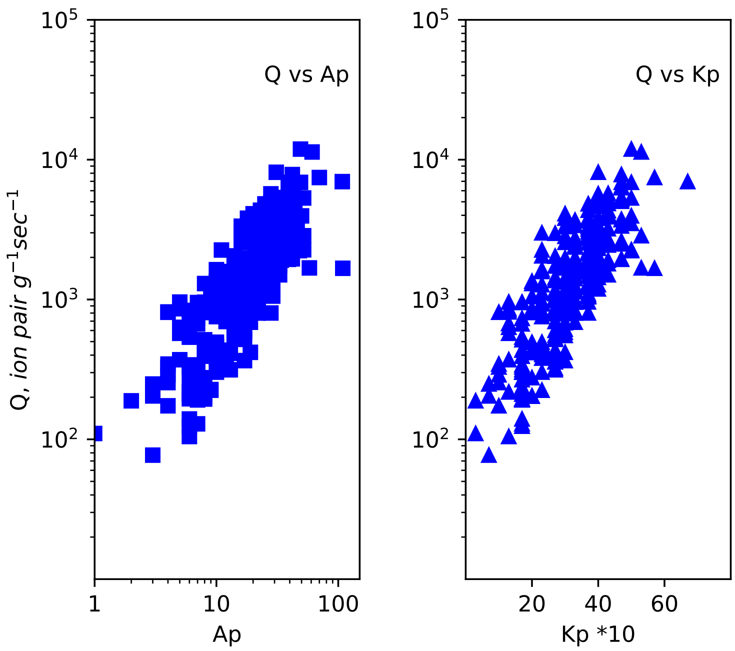

Figure 6. Ionization rates at a height of 25 km vs. Kp and Ap index. Blue squares and blue triangles—EEP ionization rates based on MEPED POES data. The square—EEP ionization rates vs. Ap. The triangle—EEP ionization rates vs. Kp.

6. Summary and Discussion

EEPs are of great practical importance, because the additional ionization caused by them affects the processes in the Earth's atmosphere. It remains unknown what fraction of the electrons of the outer belt drops out to the atmosphere, and what fraction goes into interplanetary space. Little is known about the spatial dimensions of the EEP. Ideally, there would be many balloons constantly monitoring the EEA throughout the auroral zone. At present, we have rather rare results of balloon observations in one geographical location, which do not allow us to fix the EEP duration and do not always provide reliable information about the energy spectrum of electrons. Comparing the results of observations on the POES satellites and balloons, we proposed a criterion by which it is possible to monitor the ionization in the atmosphere at altitudes down to 20–25 km using measurements on satellites. Applying this criterion, namely that the >800 keV electron flux should be >100 pfu, to the data of POES 15, 16, and 17 for 2003, we estimated the number of days when EEP would be observed in the northern polar zone (geographic latitude 60°–70°, longitude 0°–360°, McIlwain parameter L = 4–8). There were 279 such days, but EEP duration was more than 15 min in 145 cases, and more than 30 min only in 33 cases. The distribution of the found EEP events over 2003 is consistent with variations in the >2 MeV electron fluence in the outer radiation belt. A reasonable correlation of the obtained ionization rates in the atmosphere at a height of 25 km with the geomagnetic index confirms that the proposed criterion enables finding days when strong EEPs occur. This indicates the plausibility of the proposed criterion and makes it possible to evaluate the ionization situation in the stratosphere at auroral latitudes from day to day. Such an estimate is only the first approach to understanding the role of constantly precipitating electrons from the outer radiation belt in the ionization of the atmosphere. In the future, we hope to find a better match between satellite observations and ionization at stratospheric altitudes.

Author Contributions: Conceptualization: I.M. and G.B.; spectra retrieval: G.B., V.M. and I.M.; ionization rate computation: A.M. and I.M.; visualization of all results: A.M., I.M. and N.B.; balloon observation: V.M. and G.B.; writing—original draft preparation: I.M. and G.B. All authors have read and agreed to the published version of the manuscript.

Funding: Ministry of Science and Higher Education of the Russian Federation under agreement 075-15-2021-583 and project RSF No. 22-62-00048 in the frame of the task "Atmospheric effects of precipitation of energetic electrons from the outer radiation belt: Part II".

Data Availability Statement: NOAA POES data: https://www.ngdc.noaa.gov/stp/satellite/poes/index.html (last accessed on 18 June 2023). Geomagnetic indices: https://omniweb.gsfc.nasa.gov/cgi/nx1.cgi (last accessed on 18 June 2023). LPI catalog of precipitating electrons: http://sites.lebedev.ru/en/DNS_FIAN/479.html (last accessed on 18 June 2023). Radiation belt with electrons of more than 2 MeV: http://www.ngdc.noaa.gov/stp/solar/sateenvi.html (last accessed on 18 June 2023). All spectra and ionization rates are available upon request from I.M.

Acknowledgments: The work of A.M. and N.B. was supported by the "Laboratory for the study of the ozone layer and the upper atmosphere" of the Ministry of Science and Higher Education of the Russian Federation under agreement 075-15-2021-583. The work of I.M. and G.B. was supported by a grant from the Russian Science Foundation (project RSF No. 22-62-00048) in the frame of the task "Atmospheric effects of precipitation of energetic electrons from the outer radiation belt: Part II".

Conflicts of Interest: The authors declare no conflict of interest.

References

1. Lyons, L.R.; Thorne, R.M. Equilibrium structure of radiation belt electrons. *Geophys. Res. Lett.* **1973**, *78*, 2142–2149. [CrossRef]
2. Reeves, G.D.; McAdams, K.L.; Friedel, R.H.W.; O'Brien, T.P. Acceleration and loss of relativistic electrons during geomagnetic storms. *Geophys. Res. Lett.* **2003**, *30*, 1529. [CrossRef]
3. Millan, R.M.; Thorne, R.M. Review of radiation belt relativistic electron losses. *J. Atmos. Sol.-Terr. Phys.* **2007**, *69*, 362–377. [CrossRef]
4. Ukhorskiy, A.Y.; Anderson, B.J.; Brandt, P.C.; Tsyganenko, N.A. Storm time evolution of the outer radiation belt: Transport and losses. *J. Geophys. Res. Space Phys.* **2006**, *111*, A11S03. [CrossRef]
5. McDowell, J.C. The edge of space: Revisiting the Karman Line. *Acta Astronaut.* **2018**, *151*, 668–677. [CrossRef]
6. Porter, H.S.; Jackman, C.H.; Green, A.E.S. Efficiencies for production of atomic nitrogen and oxygen by relativistic proton impact in air. *J. Chem. Phys.* **1976**, *65*, 154–167. [CrossRef]
7. Solomon, S.; Rusch, D.W.; Gerard, J.C.; Reid, G.C.; Crutzen, P.J. The effect of particle precipitation events on the neutral and ion chemistry of the middle atmosphere: II. Odd hydrogen. *Planet. Space Sci* **1981**, *29*, 885–893. [CrossRef]
8. Brasseur, G.P.; Solomon, S. *Aeronomy of the Middle Atmosphere: Chemistry and Physics of the Stratosphere and Mesosphere*; Springer Science and Business Media: Berlin, Germany, 2009.
9. Rozanov, E.; Calisto, M.; Egorova, T.; Peter, T.; Schmutz, W. Influence of the Precipitating Energetic Particles on Atmospheric Chemistry and Climate. *Surv. Geophys.* **2012**, *33*, 483–501. [CrossRef]
10. Sinnhuber, M.; Nieder, H.; Wieters, N. Energetic Particle Precipitation and the Chemistry of the Mesosphere/Lower Thermosphere. *Surv. Geophys.* **2012**, *33*, 1281–1334. [CrossRef]
11. Mironova, I.A.; Aplin, K.L.; Arnold, F.; Bazilevskaya, G.A.; Harrison, R.G.; Krivolutsky, A.A.; Nicoll, K.A.; Rozanov, E.V.; Turunen, E.; Usoskin, I.G. Energetic Particle Influence on the Earth's Atmosphere. *Space Sci. Rev.* **2015**, *194*, 1–96. [CrossRef]
12. Mironova, I.; Sinnhuber, M.; Bazilevskaya, G.; Clilverd, M.; Funke, B.; Makhmutov, V.; Rozanov, E.; Santee, M.L.; Sukhodolov, T.; Ulich, T. Exceptional middle latitude electron precipitation detected by balloon observations: Implications for atmospheric composition. *Atm. Chem. Phys.* **2022**, *22*, 6703–6716. [CrossRef]
13. Grankin, D.; Mironova, I.; Bazilevskaya, G.; Rozanov, E.; Egorova, T. Atmospheric Response to EEP during Geomagnetic Disturbances. *Atmosphere* **2023**, *14*, 273. [CrossRef]

14. Pettit, J.; Elliott, S.; Randall, C.; Halford, A.; Jaynes, A.; Garcia-Sage, K. Investigation of the drivers and atmospheric impacts of energetic electron precipitation. *Front. Astron. Space Sci.* **2023**, *10*, 1162564. [CrossRef]
15. Mironova, I.A.; Artamonov, A.A.; Bazilevskaya, G.A.; Rozanov, E.V.; Kovaltsov, G.A.; Makhmutov, V.S.; Mishev, A.L.; Karagodin, A.V. Ionization of the Polar Atmosphere by Energetic Electron Precipitation Retrieved From Balloon Measurements. *Geophys. Res. Lett.* **2019**, *46*, 990–996. [CrossRef]
16. Nesse Tyssøy, H.; Sinnhuber, M.; Asikainen, T.; Bender, S.; Clilverd, M.A.; Funke, B.; van de Kamp, M.; Pettit, J.M.; Randall, C.E.; Reddmann, T.; et al. HEPPA III Intercomparison Experiment on Electron Precipitation Impacts: 1. Estimated Ionization Rates During a Geomagnetic Active Period in April 2010. *J. Geophys. Res. Space Phys.* **2022**, *127*, e29128. [CrossRef]
17. Makhmutov, V.S.; Bazilevskaya, G.A.; Stozhkov, Y.I.; Svirzhevskaya, A.K.; Svirzhevsky, N.S. Catalogue of electron precipitation events as observed in the long-duration cosmic ray balloon experiment. *J. Atmos. Sol.-Terr. Phys.* **2016**, *149*, 258–276. [CrossRef]
18. Bazilevskaya, G.A.; Kalinin, M.S.; Krainev, M.B.; Makhmutov, V.S.; Stozhkov, Y.I.; Svirzhevskaya, A.K.; Svirzhevsky, N.S.; Gvozdevsky, B.B. Temporal Characteristics of Energetic Magnetospheric Electron Precipitation as Observed During Long-Term Balloon Observations. *J. Geophys. Res. Space Phys.* **2020**, *125*, e28033. [CrossRef]
19. Millan, R.M.; Lin, R.P.; Smith, D.M.; Lorentzen, K.R.; McCarthy, M.P. X-ray observations of MeV electron precipitation with a balloon-borne germanium spectrometer. *Geophys. Res. Lett.* **2002**, *29*, 2194. [CrossRef]
20. Mironova, I.; Bazilevskaya, G.; Kovaltsov, G.; Artamonov, A.; Rozanov, E.; Mishev, A.; Makhmutov, V.; Karagodin, A.; Golubenko, K. Spectra of high energy electron precipitation and atmospheric ionization rates retrieval from balloon measurements. *Sci. Total Environ.* **2019**, *693*, 133242. [CrossRef]
21. Stozhkov, Y.I.; Svirzhevsky, N.S.; Bazilevskaya, G.A.; Kvashnin, A.N.; Makhmutov, V.S.; Svirzhevskaya, A.K. Long-term (50 years) measurements of cosmic ray fluxes in the atmosphere. *Adv. Space Res.* **2009**, *44*, 1124–1137. [CrossRef]
22. Bazilevskaya, G.A.; Kalinin, M.S.; Krainev, M.B.; Makhmutov, V.S.; Svirzhevskaya, A.K.; Svirzhevsky, N.S.; Stozhkov, Y.I.; Gvozdevsky, B.B. Characteristics of the Energetic Electron Precipitation and Magnetospheric Conditions in 1994. *Geomagn. Aeron.* **2018**, *58*, 483–492. [CrossRef]
23. Clilverd, M.A.; Rodger, C.J.; Moffat-Griffin, T.; Spanswick, E.; Breen, P.; Menk, F.W.; Grew, R.S.; Hayashi, K.; Mann, I.R. Energetic outer radiation belt electron precipitation during recurrent solar activity. *J. Geophys. Res. Space Phys.* **2010**, *115*, A08323. [CrossRef]
24. Rodger, C.J.; Clilverd, M.A.; Green, J.C.; Lam, M.M. Use of POES SEM-2 observations to examine radiation belt dynamics and energetic electron precipitation into the atmosphere. *J. Geophys. Res. Space Phys.* **2010**, *115*, A04202. [CrossRef]
25. Yahnin, A.G.; Yahnina, T.A.; Raita, T.; Manninen, J. Ground pulsation magnetometer observations conjugated with relativistic electron precipitation. *J. Geophys. Res. Space Phys.* **2017**, *122*, 9169–9182. [CrossRef]
26. Bazilevskaya, G.A.; Dyusembekova, A.S.; Kalinin, M.S.; Krainev, M.B.; Makhmutov, V.S.; Svirzhevskaya, A.K.; Svirzhevsky, N.S.; Stozhkov, Y.I.; Tulekov, E.A. Comparison of the Results on Precipitation of High-Energy Electrons in the Stratosphere and on Satellites. *Cosm. Res.* **2021**, *59*, 24–29. [CrossRef]
27. Bazilevskaya, G.A.; Kalinin, M.S.; Krainev, M.B.; Makhmutov, V.S.; Svirzhevskaya, A.K.; Svirzhevsky, N.S.; Stozhkov, Y.I.; Philippov, M.V.; Balabin, Y.V.; Gvozdevsky, B.B. Precipitation of magnetospheric electrons into the Earth's atmosphere and the electrons of the outer radiation belt. *Bull. Russ. Acad. Sci. Phys.* **2017**, *81*, 215–218. [CrossRef]
28. Fang, X.; Randall, C.E.; Lummerzheim, D.; Wang, W.; Lu, G.; Solomon, S.C.; Frahm, R.A. Parameterization of monoenergetic electron impact ionization. *Geophys. Res. Lett.* **2010**, *37*, L22106. [CrossRef]
29. Mironova, I.; Kovaltsov, G.; Mishev, A.; Artamonov, A. Ionization in the Earth's Atmosphere Due to Isotropic Energetic Electron Precipitation: Ion Production and Primary Electron Spectra. *Remote Sens.* **2021**, *13*, 4161. [CrossRef]
30. Comess, M.D.; Smith, D.M.; Selesnick, R.S.; Millan, R.M.; Sample, J.G. Duskside relativistic electron precipitation as measured by SAMPEX: A statistical survey. *J. Geophys. Res.* **2013**, *118*, 5050–5058. [CrossRef]
31. Whittaker, I.C.; Gamble, R.J.; Rodger, C.J.; Clilverd, M.A.; Sauvaud, J.A. Determining the spectra of radiation belt electron losses: Fitting DEMETER electron flux observations for typical and storm times. *J. Geophys. Res. Space Phys.* **2013**, *118*, 7611–7623. [CrossRef]